IEEE Access
Multidisciplinary | Rapid Review | Open Access Journal

Received September 25, 2020, accepted October 20, 2020, date of publication October 23, 2020, date of current version November 9, 2020.

Digital Object Identifier 10.1109/ACCESS.2020.3033404

Efficiency Estimation of Synchronous Generators for Marine Applications and Verification With Shop Trial Data and Real Ship Operation Data

HIROYASU KIFUNE[1], (Member, IEEE), MEHDI KARBALAYE ZADHE[2], (Member, IEEE), AND HIDETSUGU SASAKI[1]

[1]Department of Marine Electronics and Mechanical Engineering, Tokyo University of Marine Science and Technology, Tokyo 1358533, Japan
[2]Department of Marine Technology, Norwegian University of Science and Technology, 7028 Trondheim, Norway

Corresponding author: Hiroyasu Kifune (kifune@kaiyodai.ac.jp)

This work was supported in part by the JSPS KAKENHI under Grant JP18K04579.

ABSTRACT Three methods were explored to estimate the efficiency for the conversion of mechanical power to electrical power using synchronous generators in ships at low power factors. Generally, the generator efficiency data is provided by manufacturers as shop trial data and is measured by operating generators under power factor of 0.8 and 1.0. However, the efficiency of synchronous generators is not measured under low power factor of less than 0.8. In practice, onboard generators occasionally operate at low power factor and it is desirable to clarify their characteristics for power system designers of large vessels. By substituting the shop trial data into the proposed efficiency estimation formulas, the generator efficiency at low power factor was extrapolated. To evaluate the validity of these methods, the fuel consumption characteristics of diesel engines as prime movers was focused. The estimation of the generator efficiency was indirectly validated using a statistical analysis of long-term observational data of the generator in operation. As a result, the efficiency estimation method based on a power loss mechanism gave the most reliable result among the three estimation methods. The root mean squared error of the calculated specific fuel consumption was 3.5 g/kWh, which is approximately 1.66 % error rate.

INDEX TERMS Synchronous generator, efficiency estimation, specific fuel consumption, marine propulsion.

I. INTRODUCTION

A. DEVELOPMENT OF MARINE DIESEL ELECTRIC

Diesel electric and hybrid powertrains are becomming more commonly used in various vehicles to reduce fuel consumption [1]–[5]. In large marine vessels, electric propulsion is composed of diesel engines, synchronous generators, electric machines for power take-in (PTI)/power take-off (PTO) [6], [7], optional AC-DC or DC-AC converters [8]–[10], steam turbines for recovering the thermal energy from exhaust gas [11], [12], and lithium-ion batteries for energy storage [13]–[15]. Proper management of the energy flow is necessary to achieve optimal fuel efficiency [5], [7], [14]–[17]. In the same manner as a hybrid car [18], engine speed control based on the torque-speed map [7], [17] is a key parameter for reducing fuel consumption. Unlike automotive powertrains, large vessel power systems cannot be easily built to test and evaluate performance due to their large size and cost. Hence, in the marine industry, several simulation methods have been discussed for designing the control, testing, evaluation, and optimization of power systems [7], [19]–[22].

The associate editor coordinating the review of this manuscript and approving it for publication was Xiaodong Liang.

B. PREVIOUS WORK

To evaluate the fuel economy of power system, it is necessary to obtain the appropriate energy conversion efficiency characteristics of each system. In case of diesel engines, the specific fuel consumption (SFC) is evaluated. Other examples include the mechanical to electrical power conversion efficiency of synchronous generators, the electric power conversion efficiency of AC/DC, DC/DC, and DC/AC converters, the electrical to mechanical power conversion efficiency of electric motors, and the transmission efficiency of gears for the power system designers.

The SFC of a diesel engine as the prime mover of a genset has been discussed to optimize the fuel consumption in marine hybrid and electric power system [7], [17], [23], [24]. The SFC can be improved by controlling the engine speed according to the load factor. DC power system allow the generators to operate at a variable speed and give flexibility to the electrical system design [25]. To realize variable speed generator for fuel reduction, the three-phase AC electric power of synchronous generators is converted into DC power by employing DC-AC converters, which is then supplied to the DC bus [26]. The Power factor, total harmonic distortion, and voltage regulation function can be improved by using active front end converters when DC electrical systems are used as the power distribution system [27]. However, there was no detailed analysis of the energy dissipation of the generators, converters, and electric machines in these systems. When evaluating the difference between AC and DC distributions in terms of efficiency, it is necessary to clarify the relationship between the power factor of the onboard AC electrical system and the efficiency of the synchronous generator.

Reference [22] introduced a method to calculate the power loss of a synchronous generator theoretically from the ratio of the active power to the reactive power. The parameters required in the calculation were taken from [28], which simulates the voltage response to load changes, but the power loss is not detailed. In addition, the calculations require parameters that cannot be obtained from general shop trial data that is measured by maker to prove product performance.

Reference [7] regarded the generator efficiency as a function of the load factor and its shaft speed, and the entire calculation is conducted on an effective power basis. However, the effects of the power factor of the synchronous generator has not been investigated.

Generally, the power factor on an onboard electrical system is lower than the power factor of an onshore power system, and the improvement target is 0.8-0.9 [29]. Reference [21], [29] discussed the reactive power compensation of onboard electrical systems to improve fuel consumption through several case studies. However, there was no mention of the relationship between the efficiency of a synchronous generator and its power factor. As will be described later, the synchronous generator occasionally operates at a low power factor under a low load condition in a marine vessel's electric system [30], which increases power loss due to an increase in the reactive current.

To enable power system designers and researchers to determine the proper energy flow, it is desirable to obtain detailed efficiency maps of a synchronous generator in terms of the load factor and the power factor. In the industry, energy losses and efficiencies of the rotating electrical machines are measured complying with IEC 60034-2-1 standards [31]. Experimental methods of measuring energy loss and simulations of the finite element method to evaluate energy loss in synchronous machines have been proposed and discussed in various studies such as [32]–[35]. These analyses can be conducted at the development stage of the synchronous generator, but not at the design stage of the marine onboard electrical power system. Even if the power factor can vary over a wide range, power system designers are forced to use the efficiency values that were measured at high power factors, which means that the power system may perform different from their intent.

C. CONTRIBUTION

To serve those who need to measure a generator's efficiency at low power factors and wide load factors, this article presents an efficiency estimation method using the limited information provided by a manufacturer to estimate the efficiency of large onboard synchronous generators, which have not been investigated before. These formulas can be used with the data found in general shop test data, unlike [22]. Three extrapolation methods for estimating the efficiency under low power factors are discussed. These estimation methods were evaluated using long-term observational data from the actual onboard diesel engine generators and were compared to determine the most accurate method. To eliminate the effects of load fluctuations on the prime mover engine, coefficient value filters were introduced and evaluated with statistical analysis. The results of the estimation were validated with shop trial data and actual operating data to demonstrate the effectiveness of the proposed estimation method.

II. THEORETICAL METHOD FOR ESTIMATING EFFICIENCY OF GENERATOR

A. SHOP TRIAL DATA

It is assumed that the load factor x and the power factor $\cos\theta$ are primary factors that determine the generator efficiency η, as in (1) below.

$$\eta = f(x, cos\theta) \tag{1}$$

An efficiency map can be approximated using several efficiency data on the plane of x and $\cos\theta$.

Table 1 shows the specifications of the synchronous generator used to evaluate the proposed methods for estimating the efficiency values. In general, power system designers have access to all equipment parameters in a datasheet called "shop trial data," which includes ratings, input/output conditions, and efficiency, as shown in Table 1. Generally, the manufacturer provides efficiency data at several load conditions (x = 25%, 50%, 75%, and 100%) and, in some cases, efficiency at overload conditions (e.g., 110%, 125%, and 150%) are provided as additional information.

Fig. 1 shows a typical and simplified onboard three-phase AC electrical power system for large cargo vessels such as container ships, liquified natural gas carriers, crude oil carriers, and bulk carriers. Generally, two or more gensets which is consist of a diesel engine and a synchronous generator are installed to meet onboard demand. Turbo charged, four-cycle, and medium-high speed diesel engines are usually employed as the prime movers. Most electric loads are induction motors for various pumps and are often driven at 60 Hz without an

TABLE 1. Excerpt of shop trial data of an onboard synchronous generator.

Ratings and specifications						
Voltage		450 V				
Current		1203 A				
Frequency		60 Hz				
Phase		3				
Pole		8				
Speed		900 rpm				
Efficiency						
Load factor, %		25	50	75	100	125
Power factor	0.8	89.7	93.1	93.7	93.5	93.0
	1.0	90.6	94.3	95.3	95.5	95.5

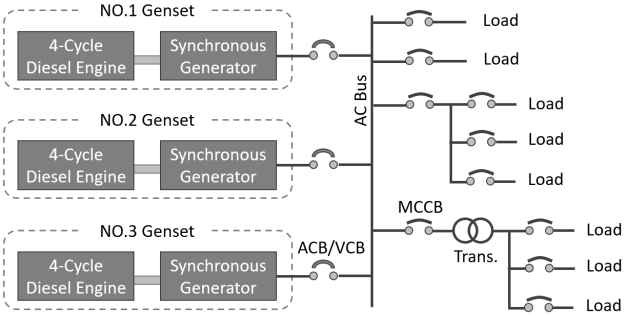

FIGURE 1. Single line diagram of typical and simplified AC electrical power system on board.

inverter. Therefore, the power factor of onboard AC electrical system is usually lower than onshore electrical system.

Since onboard electrical systems are generally assumed to operate at a power factor of around 0.8, manufacturers measure or calculate a generator's efficiency at power factors of 1 and 0.8. Therefore, the efficiency η is approximated as a two-parameter polynomial function with load factor x and power factor $\cos\theta$.

B. VALIDATION METHOD

The Efficiency η is smoothly approximated as a polynomial function in the coordinate of the load factor x using the shop trial data shown in Table 1. Unfortunately, only two data are available at the coordinate of the power factor $\cos\theta$ to create the efficiency approximation functions. The approximated polynomial is, in principle, a linear function.

To evaluate the approximation methods, the actual operating data of the onboard gensets under various loads and power factors was analyzed over a period of six months. The efficiency of a generator η is the ratio of the electrical power P_{gen} to the mechanical power which is often called as the BHP (brake horse power) of the prime mover engine, as in (2).

$$\eta = \frac{P_{gen}}{BHP} = \frac{60P_{gen}}{2\pi NT} \tag{2}$$

where, N[rpm] is speed and T[Nm] is the torque on the shaft between the diesel engine and the synchronous generator. P_{gen} was obtained from the actual onboard observation data. It was difficult to add a torque sensor to measure T because the data were collected from onboard gensets which were already installed without the torque sensor. It was not practical to add a loadcell between the engine and the synchronous generator due to the narrow space. Even if a loadcell could be physically installed, natural frequency which is often called as the critical speed of the shaft system including a coupling device and a flywheel may render the data inadequate for actual marine gensets. Therefore, BHP was determined indirectly by implementing statistical analysis as described later in Section III. The estimated efficiency values of the synchronous generator were evaluated after considering BHP and fuel consumption characteristics of the diesel engine.

C. LINEAR EFFICIENCY APPROXIMATION

With power factors of 1 and 0.8, the efficiencies under five load factor conditions (x = 25%, 50%, 75%, 100%, and 125%) are already known (see Table 1). The simplest extrapolation was to fit the relationship between the power factor 1.0 and 0.8 linearly to the low power factor region. If the load factor x is at a certain value x_g, it is assumed that the efficiency η is a linear function of the power factor with slope a_{xg} and intercept b_{xg}.

$$\eta(x_g, cos\theta) = a_{xg}cos\theta + b_{xg} \tag{3}$$

Fig. 2 shows the extrapolation results based on (3). In this case, since there were five approximation formulas, five efficiency values were obtained under specific power factor conditions ($\cos\theta = q$). A polynomial approximation formula can be expressed as a function of the load factor x based on these estimated values. The formulas fit well to a fourth-order polynomial approximation, as shown in Fig. 3.

$$\eta(x, q) = Ax^4 + Bx^3 + Cx^2 + Dx + E \tag{4}$$

Coefficient values A to E can be determined by five approximation formulas (4). Implementing interpolation and extrapolation using these approximation formulas yielded an efficiency map in terms of the load factor x and power factor $\cos\theta$ (see Fig. 4).

D. LINEAR APPROXIMATION OF POWER LOSS

By rearranging (2), BHP can be expressed as follows:

$$BHP = P_{gen}/\eta$$

Then, the power loss P_{loss} of the generator under the given conditions can be obtained using (5)

$$P_{loss}(x_g, cos\theta) = a_{xg}cos\theta + b_{xg} \tag{5}$$

When the load factor x is equal to the certain value x_g, the power loss of the generator P_{loss} is a linear function of the power factor with slope a_{xg} and intercept b_{xg} as shown in (6).

$$P_{loss} = BHP - P_{gen} = (\frac{1}{\eta} - 1)P_{gen} \tag{6}$$

Fig. 5 shows the approximation lines used for extrapolating to the low power factor region. Using these approximation

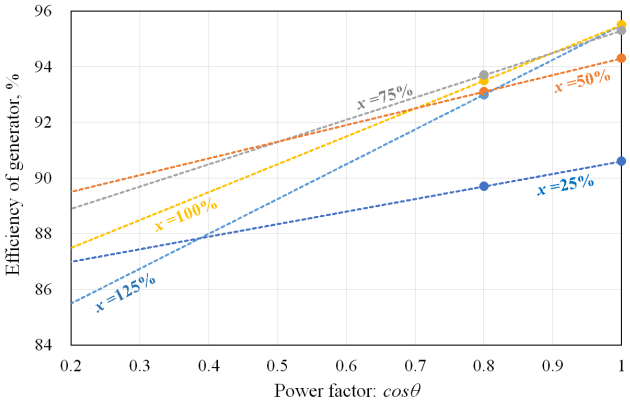

FIGURE 2. Extrapolation to the low power factor area by implementing a linear approximation of efficiency given in shop trial data.

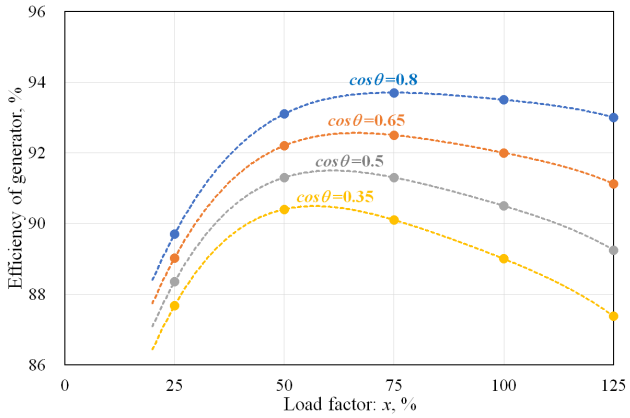

FIGURE 3. Polynomial approximation of efficiency as a function of load factor.

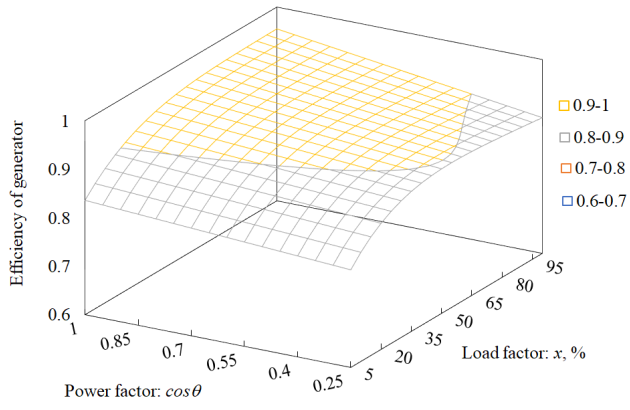

FIGURE 4. Efficiency map estimated by linear approximation of efficiency given in shop trial data.

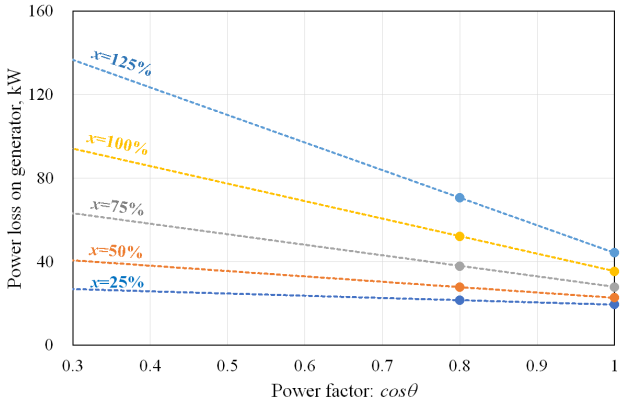

FIGURE 5. Extrapolation to the low power factor region by implementing linear approximation of the generator power loss.

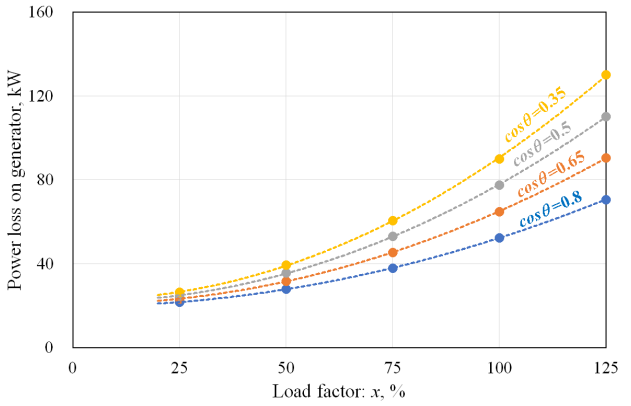

FIGURE 6. Polynomial approximation of power loss as a function of load factor.

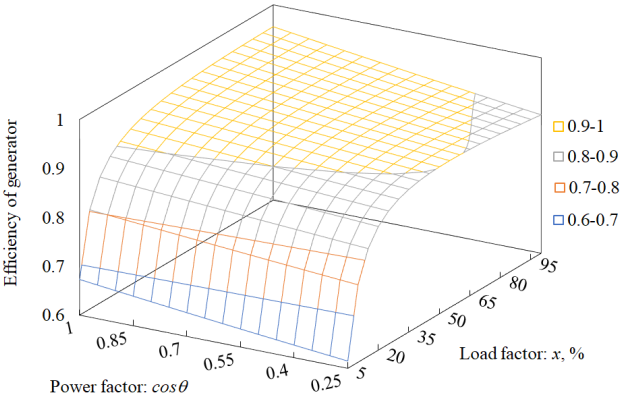

FIGURE 7. Efficiency map estimated by linear approximation of power loss.

formulas, the power loss P_{loss} was estimated at a low power factor. In this case, because there are five approximation formulas, five power loss values were obtained under a given power factor condition ($\cos\theta = q$). A polynomial approximation formula was given as a function of the load factor x based on these estimated values. In this case, the formulas fit well to a second-order polynomial approximation (see Fig. 6).

$$P_{loss}(x, q) = Ax^2 + Bx + C \tag{7}$$

Implementing both interpolation and extrapolation using these approximation formulas yielded an efficiency map in

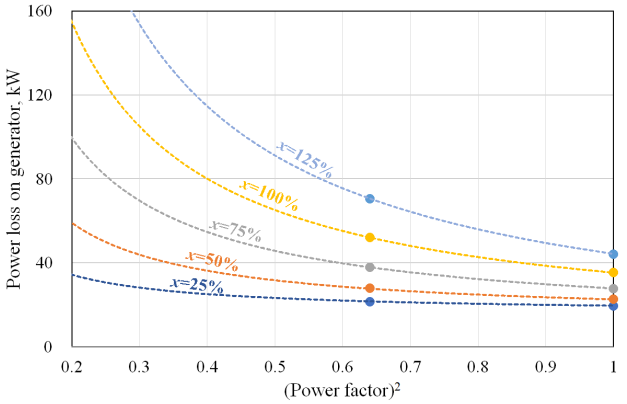

FIGURE 8. Extrapolation to the low power factor region by implementing an approximation based on the energy dissipation mechanism of synchronous generator.

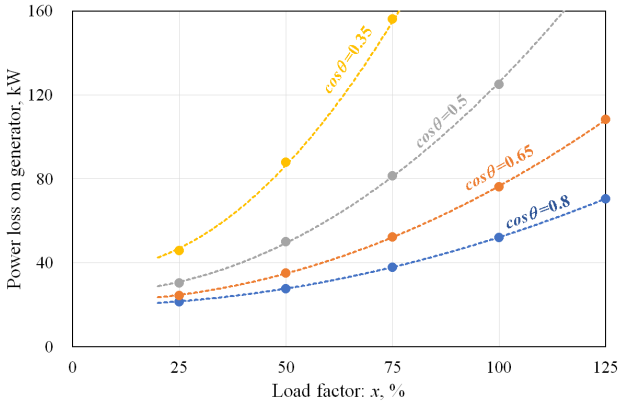

FIGURE 9. Polynomial approximation based on energy dissipation mechanism as a function of load factor.

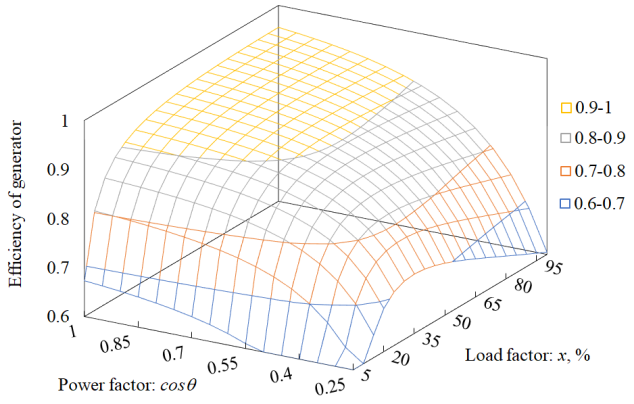

FIGURE 10. Efficiency map estimated by the energy dissipation mechanism of synchronous generator.

terms of the load factor x and the power factor cosθ (see Fig. 7). The map shows that the efficiency was significantly reduced under low load conditions.

E. POWER LOSS APPROXIMATION BASED ON ENERGY DISSIPATION MODEL

It is reasonable to consider the mechanism of the power loss to increase the accuracy of the model, but it should be

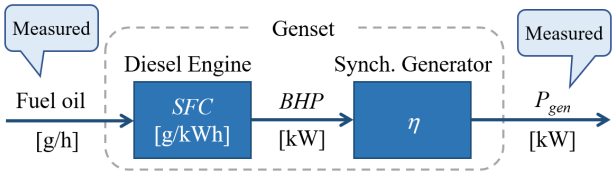

FIGURE 11. Energy conversion in diesel engine generators.

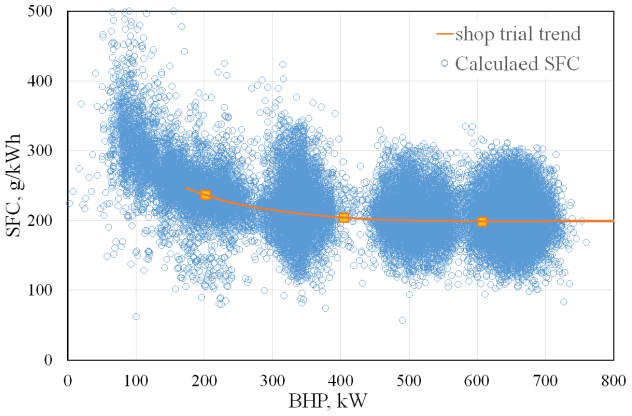

FIGURE 12. Shop trial data and SFC values calculated with an estimation method from the observed data.

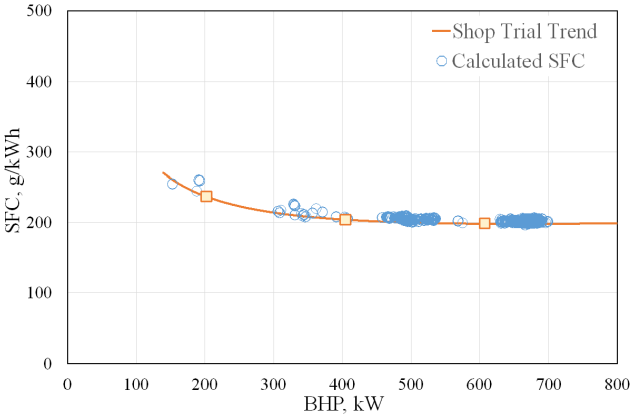

FIGURE 13. Shop trial data and extracted SFC data with CV value less than 0.01 for 10 min.

estimated over a wide power factor range. The power loss of a synchronous generator is divided into several factors, including mechanical energy loss P_m [kW], electrical energy loss usually called copper loss P_c [kW], core loss usually called iron loss P_i [kW], loss on field winding P_f [kW], and stray loss P_s [kW] [36]. The power loss of the synchronous generator P_{loss} [kW] can be simplified as follows:

$$P_{loss} = P_c + P_i + P_f + P_s + P_m \tag{8}$$

The mechanical loss P_m includes the bearing friction loss and rotor air friction loss. When electric machine operate at a constant speed, P_m is almost independent of output power [37]. A generator operates at a constant speed to supply a fixed power of 60 Hz in a general marine power system.

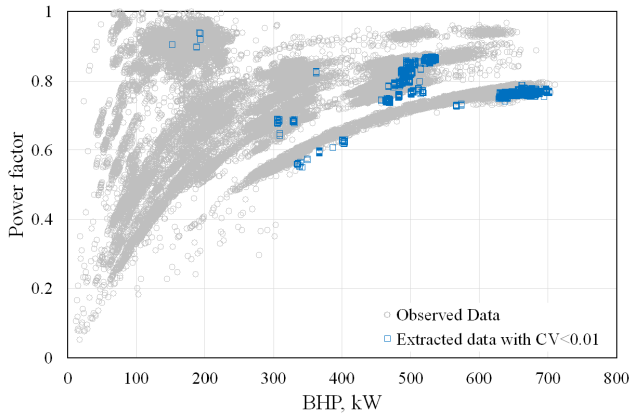

FIGURE 14. Relation between BHP and power factor in observed data.

Therefore, the mechanical loss is considered a constant value independent of the electrical conditions.

The power loss on the field coil P_f depends on the exciting current, and the value changes depending on the power factor. In a ship, since the inductive load is large and the power factor is delayed, a decrease in the power factor causes an increase in the exciting current to maintain output voltage. Therefore, the power loss in the field coil inevitably increases. However, it is small compared to the current flowing in the armature winding. For example, in the case of the generator shown in Table 1, the excitation current is 6.9 A at power factor of 0.8. The power consumption is around 0.4 kW, which corresponds to 0.05% of the generator rated power. Therefore, the power loss due to the exciting current depends on the load factor and the power factor, but its influence on the generator's efficiency is small. As a result, the power loss due to the exciting current can be regarded as a fixed loss like the mechanical loss.

The copper loss P_c of the armature conductor is caused by the load current I_L [A]. The stray loss P_s is proportional to the square of I_L [37]:

$$P_c + P_s = {I_L}^2(R_w + R_s) \cdot 10^{-3} \tag{9}$$

where, R_w [Ω] represents the resistance of the armature conductor, and R_s [Ω] represents the resistance of stray energy loss.

If the loads connected to the generator are symmetrical, the load current can be expressed as:

$$I_L = \frac{10^3 P_{gen}}{\sqrt{3} V cos\theta} \tag{10}$$

where, V [V] is the output terminal voltage of the generator. Substituting (10) into (9), the following formula is obtained:

$$\begin{aligned} P_c + P_s &= \frac{10^3 {P_{gen}}^2 (R_w + R_s)}{3V^2 cos^2\theta} \\ &= \frac{{P_{rating}}^2 (R_w + R_s)}{30V^2} \cdot \frac{x^2}{cos^2\theta} \end{aligned} \tag{11}$$

where, P_{rating} [kW] is the rating power of the generator, and x [%] is the load factor ($0 \leq x \leq 100$) of the generator, defined as $100\ P_{gen}/P_{rating}$.

These losses are expressed as a function of square of the power factor. The iron loss P_i can be divided into the hysteresis loss P_h [kW] and the eddy current loss P_e [kW]. P_h depends on the maximum flux density B_m [T], frequency f [Hz], the quality of the steel, and the size of the armature:

$$P_h = 10^{-3} k_h f {B_m}^n \tag{12}$$

where, k_h and n are empirically derived constants for a given material. The value of n is typically in the range of 1.5 to 2.5, and 1.6 is often used for estimation [36], [38].

Eddy current loss P_e in the armature is expressed as:

$$P_e = 10^{-3} k_e (t_m f B_m)^2 \tag{13}$$

where, k_e is an empirically a derived constant for a given material, and t_m [m] is the material thickness.

According to the armature reaction theory, the main field flux is weakened by a lagging power factor. To maintain a constant output terminal voltage, it is necessary to hold the synthetic magnetic flux of the main field flux and the armature flux at the same level by adjusting the magnitude of main field flux. Therefore, the maximum value of the synthetic flux B_m can be assumed to be constant, regardless of the power factor and the load factor conditions. In other words, the iron loss is nearly constant value.

Therefore, the generator power loss P_{loss} with respect to the load factor x and the power factor $cos\theta$ can be expressed as follows:

$$\begin{aligned} P_{loss}(x, cos\theta) = {} & \frac{{P_{rating}}^2 (R_w + R_s)}{30V^2} \cdot \frac{x^2}{cos^2\theta} \\ & + 10^{-3} k_h f {B_m}^n + 10^{-3} k_e (t_m f B_m)^2 + P_f + P_m \end{aligned} \tag{14}$$

In addition, if the load factor x is equal to a given value of x_g, the function can be simplified as (15).

$$P_{loss}(x_g, cos\theta) = a_{xg} \frac{1}{cos^2\theta} + b_{xg} \tag{15}$$

where,

$$\begin{aligned} a_{xg} &= \frac{{P_{rating}}^2 (R_w + R_s) {x_g}^2}{30V^2} \\ b_{xg} &= 10^{-3} k_h f {B_m}^n + 10^{-3} k_e (t_m f B_m)^2 + P_f + P_m \end{aligned}$$

The coefficient values (a_{xg} and b_{xg}) can be determined based on the values given in Table 1. The approximation lines can be drawn to extrapolate to the low power factor region, as shown in Fig. 8. The power loss P_{loss} can be estimated under low power factor conditions using these approximation formulas. In this case, since there were five approximation formulas, we obtained five values of the power loss under a given power factor condition ($cos\theta = q$). A polynomial approximation formula is given as a function of the load

factor x based on these estimated values. The formula fits well to a second-order polynomial approximation (see Fig. 9):

$$P_{loss}(x, q) = Ax^2 + Bx + C \tag{16}$$

Based on these estimates, the power loss increases significantly at low power factor conditions. Implementing both interpolation and extrapolation using these approximation formulas, an efficiency map in terms of load factor x and power factor $\cos\theta$ can be obtained (see Fig. 10). The map shows that efficiency decreases both in low load factor conditions and in low power factor conditions.

III. EXPERIMENTAL ANALYSIS AND VALIDATION

A. CALCULATION OF SFC

To evaluate the estimated efficiency η_{gen} of the synchronous generator, it is necessary to know the BHP of the prime mover (see Fig. 11). However, due to the limited space between the engine and the generator, it was not possible to install sensors to measure the torque of the diesel engine. The SFC (specific fuel oil consumption) [g/kWh] of diesel engines was obtained from the shop trial data provided by the engine manufacturers. In this research, the fuel oil flow rate F_L [L/h] of the diesel engine and the output electric power P_{gen} [kW] of the synchronous generator were observed. Additionally, the characteristics of the fuel oil on the ship were examined, including oil temperature, lower heating value Q_{low} [MJ/kg], and representative oil density ρ [g/cm^3] at 15°C for converting the volumetric flow rate F_L to the mass flow rate F_g [g/h] complying with ISO 91-1 [39] standards.

$$F_g = 1000\rho k \frac{Q_{low}}{Q_s} F_L \tag{17}$$

where, Q_s is the standard lower heating value of fuel oil (= 42.7 MJ/kg) and k is a volume correction factor for the fuel oil temperature in the flow meter.

Consequently, the SFC was calculated according to (18).

$$SFC = \frac{F_g}{BHP} = \frac{\eta F_g}{P_{gen}} \tag{18}$$

The estimated efficiency η of the synchronous generator was calculated according to Fig. 4, Fig. 7, and Fig. 10. By comparing the calculated SFCs with the shop trial data of the diesel engines, it is possible to evaluate the validity of the estimation methods.

Fig. 12 shows the relationship between the BHP and the SFCs for diesel engines. The solid line follows the SFC trend provided by the shop trial data for diesel engines. The circles show the calculated SFC based on the measured fuel flow rate, electric power, and the estimated efficiency shown in Fig. 5. The calculated SFC preferably followed the SFC trend in the datasheet. However, these calculated SFCs varied considerably when compared to the shop trial trend. The variations of the calculated SFC to the shop trial trend were almost same when the efficiency map shown in Fig.7 and 10 were used for calculating SFC.

B. FILTERING VARIATION WITH CV

A shop trial is generally conducted under stable and constant load conditions. To maintain the heat balance of the diesel engine, all data including electrical power, fuel flow rate, fuel oil temperature, intake air pressure, and many other parameters are measured and averaged over approximately 30 minutes. The heat balance of an internal combustion engine is one of the most important factors in determining its SFC characteristics. For this reason, shop trials are generally performed by engine manufacturers to measure the SFC characteristics under ideal and stable load conditions using special test facilities because large marine diesel engines have large thermal capacities and delayed turbochargers. Many previous studies on diesel engines have shown that the thermal efficiency is different under transient load conditions versus steady constant load conditions [40]–[43].

In this article, actual operating data that varied significantly depending on onboard load conditions were used. Hence, to eliminate variations due to load fluctuations, it was necessary to select the appropriate data measured under conditions corresponding to quasi-constant load conditions.

To eliminate these variations, the coefficient of variation (CV) of the BHP was calculated to extract the constant load condition.

$$CV = \frac{1}{\overline{BHP}} \sqrt{\frac{1}{T} \sum_{t=1}^{T} (BHP_t - \overline{BHP})^2} \tag{19}$$

where, the $\overline{BHP}$ is the averaged value of BHP for period T.

T was set to 30 minutes to determine the quasi-steady load condition. Any data set with a CV of 1% or more were removed. However, not enough data was available to satisfy constant load condition where $T = 30$ min. By adjusting the filter parameter from 30 to 10 min, over 2500 data sets with CVs less than 1.0 % were extracted, which were sufficient for statistical analysis.

Fig. 13 shows the relationship between the BHP and the SFC for diesel engines. The solid line represents the shop trial trend and the circles show the SFC calculated using the generator efficiency map estimated in Fig. 10. The coefficient value filter removed the variations from the observed data. The calculated results fit smoothly with the trends in the shop trial.

It is inevitable that the calculation values vary due to the following reasons:

1 Supply air temperature varied depending on the intake air temperature and the inter-cooler conditions, which affects the SFC.
2 Exhaust gas back pressure to the onboard engine differed from the shop trial conditions, which affects the SFC.
3 Turbine blades of turbochargers were fouled by exhaust gas, which increase the SFC.
4 The SFC calculation complied with ISO 3046-1 [44] standards. However, not all marine fuels have the same chemical composition, which affects the ignition performance of the engine.

TABLE 2. Performance comparison of efficiency estimation methods.

SFC calculation with (Extracted conditions)	$RMSE_A$ $CV \leq 0.01$	$RMSE_B$ $CV \leq 0.01, cos\theta \leq 0.7$
Linear approximation of efficiency [g/kWh]	5.284	7.680
Linear approximation of power loss [g/kWh]	5.191	7.495
Approximation based on energy dissipation mechanism [g/kWh]	4.930	3.501

With actual onboard gensets, it is difficult to adjust for the variations mentioned above, which results in errors in the SFC calculation as described later.

C. COMPARISON OF ESTIMATED RESULTS

After filtering the variations from the observed data, three estimation methods were compared by calculating the root mean squared error (RMSE). The SFC trend predicted by the shop trial data can be approximated as a function of the load factor x.

$$\widehat{SFC} = f(x) \tag{20}$$

When $\widehat{SFC}$ is regarded as a true function, the RMSE of each estimation method is calculated as follows:

$$RMSE = \sqrt{\frac{1}{H}\sum_{i=1}^{H}(SFC_i - \widehat{SFC})^2} \tag{21}$$

where, H is total number of calculated SFC data.

Table 2 shows the RMSEs for the three estimation methods. $RMSE_A$ was targeted for analysis on all data groups after eliminating variations with the CV filter. RMSE of the estimated SFC is around 5 g/kWh which is equivalent to an averaged error rate of 2.6 % at all estimation methods. Therefore, these methods show similar performance for estimating the efficiency of a synchronous generator.

To elucidate the difference in their performances, the SFC data extracted by CV filter was analyzed for the relationship between the BHP and the power factor. Fig. 14 shows the BHP and the power factor profiles of the observed data set. As is shown in the figure, the generator operates in a wide power factor range (depicted as circles). However, the data groups extracted under the condition that the CV was less than 0.01 were unevenly distributed (shown as squares). In addition, 96% of the data which was extracted by the CV filter had a power factor of 0.7 or higher. As mentioned earlier, there was no significant difference in the estimated efficiency under the conditions of a high-power factor and load factor among the three estimation methods (Figs. 4, 7, 10). Therefore, $RMSE_A$ is the result of comparing the estimation methods under high power factor conditions. In sum, these results have no large differences.

The $RMSE_B$ was calculated under the condition of a low power factor less than 0.7 to study the performance of each estimation method. It was found that the estimation method based on the energy dissipation model gives the closest values to the shop trial data in low power factor conditions. The $RMSE_B$ value was 3.501 g/kWh, which is equivalent to an averaged error rate of 1.66 %. In the other linear approximation methods, the $RMSE_B$ value was 7.4 g/kWh or more. The estimation accuracy of these methods tends to decrease under low power factor conditions.

In conclusion, the estimation method based on the energy dissipation mechanism is valid for obtaining the efficiency of a synchronous generator using limited shop trial data.

IV. CONCLUSION

Three methods were presented for estimating the efficiency of synchronous generators in low power factor conditions including a linear approximation of efficiency, a linear approximation of power loss, and an approximation based on an energy dissipation mechanism. These estimations were performed based on the limited information available from the shop trial data. The estimated efficiency of a synchronous generator tends to be low when it runs at low load factor with any estimation method. It deteriorates drastically at low power factor conditions by applying the approximation based on the energy dissipation mechanism. An evaluation of these methods was completed by statistical analysis of a diesel engine's SFC indirectly. After calculating the RMSE of these methods, no large difference in performance was found between them. In low power factor conditions, however, the approximation based on energy dissipation mechanism gives a low error rate (RMSE is around 3.5 g/kWh) to estimate efficiency, while other linear approximation methods perform poorly (RMSE of about 7.5 g/kWh). Consequently, the efficiency of synchronous generators can be estimated by the use of shop trial data with the presented estimation method.

Using precise torque sensor for measuring BHP of the diesel engine directly and compensating calculation results by measuring the back pressure of exhaust gas are considered as future works. Additionally, this article discussed the SFC of fixed speed conventional diesel engine generators, which are mainly used in marine diesel engine generators of small to large size vessels. The characteristics of a variable frequency diesel engine generator with AC/DC converters as energy sources for the DC bus system should be analyzed in another opportunity.

ACKNOWLEDGMENT

The authors would like to thank to Captain Toshifumi HAYASHI, Chief-Engineer Yousuke KITANO, and First-Engineer Ken KATSUMI of Shinyo Maru for supporting to collect the operational data.

REFERENCES

[1] J. Voelcker, "Top 10 tech car [fuel efficient cars]," *IEEE Spectr.*, vol. 43, no. 4, pp. 34–43, May 2006, doi: 10.1109/MSPEC.2006.1611757.

[2] B. Suh, A. Frank, Y. J. Chung, E. Y. Lee, Y. H. Chang, and S. B. Han, "Economic value and utility of a powertrain system for a plug-in parallel diesel hybrid electric bus," *Int. J. Automot. Technol.*, vol. 11, no. 4, pp. 555–563, Aug. 2010, doi: 10.1007/s12239-010-0067-4.

[3] M. Gokasan, S. Bogosyan, and D. J. Goering, "Sliding mode based power-train control for efficiency improvement in series hybrid-electric vehicles," *IEEE Trans. Power Electron.*, vol. 21, no. 3, pp. 779–790, May 2006, doi: 10.1109/TPEL.2006.872373.

[4] X. Ye, Z. Jin, X. Hu, Y. Li, and Q. Lu, "Modeling and control strategy development of a parallel hybrid electric bus," *Int. J. Automot. Technol.*, vol. 14, no. 6, pp. 971–985, Dec. 2013, doi: 10.1007/s12239-013-0107-y.

[5] E. Skjong, T. A. Johansen, M. Molinas, and A. J. Sorensen, "Approaches to economic energy management in diesel–electric marine vessels," *IEEE Trans. Transport. Electrific.*, vol. 3, no. 1, pp. 22–35, Mar. 2017, doi: 10.1109/TTE.2017.2648178.

[6] L. Leclere, C. Galmiche, N. Leboeuf, N. Velly, and G.-P. Crouzet, "A new concept of PTI/PTO for marine applications," in *Proc. IEEE Vehicle Power Propuls. Conf. (VPPC)*, Dec. 2017, pp. 1–7, doi: 10.1109/VPPC.2017.8331059.

[7] M. Jaurola, A. Hedin, S. Tikkanen, and K. Huhtala, "A TOpti simulation for finding fuel saving by optimising propulsion control and power management," *J. Mar. Sci. Technol.*, vol. 25, no. 2, pp. 411–425, Jun. 2020, doi: 10.1007/s00773-019-00651-2.

[8] D. Kumar and F. Zare, "A comprehensive review of maritime microgrids: System architectures, energy efficiency, power quality, and regulations," *IEEE Access*, vol. 7, pp. 67249–67277, 2019, doi: 10.1109/ACCESS.2019.2917082.

[9] S. Kanerva and J.-F. Hansen, "State of the art in electric propulsion—Viewpoint on redundancy," in *Proc. IEEE Electr. Ship Technol. Symp.*, Apr. 2009, pp. 499–504, doi: 10.1109/ESTS.2009.4906558.

[10] J. Fredrik Hansen and F. Wendt, "History and state of the art in commercial electric ship propulsion, integrated power systems, and future trends," *Proc. IEEE*, vol. 103, no. 12, pp. 2229–2242, Dec. 2015, doi: 10.1109/JPROC.2015.2458990.

[11] H. Nakamura, *Electric, Electronics and Automatic Systems in Year Book 2014: Progress of Marine Engineering Technology in the Year 2013*. Japan Institute of Marine Engineering, 2014. [Online]. Available: http://archive.jime.jp/e/publication/yearbook/yb/pdf14/yb14-6.pdf

[12] M. Altosole, G. Benvenuto, U. Campora, M. Laviola, and A. Trucco, "Waste heat recovery from marine gas turbines and diesel engines," *Energies*, vol. 10, no. 5, p. 718, May 2017, doi: 10.3390/en10050718.

[13] P. Jammer and J. Eldridge, "Conversion of Kotug's RT Adriaan to become Europe's first hybrid tugboat," in *Proc. Int. Tug OSV*, Barcelona Spain, vol. 3, no. 3, May 2012, pp. 209–223.

[14] E. A. Sciberras, B. Zahawi, D. J. Atkinson, A. Breijs, and J. H. van Vugt, "Managing shipboard energy: A stochastic approach special issue on marine systems electrification," *IEEE Trans. Transport. Electrific.*, vol. 2, no. 4, pp. 538–546, Dec. 2016, doi: 10.1109/TTE.2016.2587682.

[15] K. Kim, K. Park, J. Lee, K. Chun, and S.-H. Lee, "Analysis of battery/generator hybrid container ship for CO_2 reduction," *IEEE Access*, vol. 6, pp. 14537–14543, 2018, doi: 10.1109/ACCESS.2018.2814635.

[16] H. Kifune, Y. Asada, and T. Nishio, "Fuel saving effect of hybrid propulsion system—Case: Tugboat is on service," *J. JIME*, vol. 53, no. 2, pp. 99–105, 2018, doi: 10.5988/jime.53.260.

[17] R. D. Geertsma, R. R. Negenborn, K. Visser, and J. J. Hopman, "Design and control of hybrid power and propulsion systems for smart ships: A review of developments," *Appl. Energy*, vol. 194, pp. 30–54, May 2017, doi: 10.1016/j.apenergy.2017.02.060.

[18] A. Kleimaier and D. Schröder, "Optimized design and control of a hybrid vehicle with CVT," *Proc. IFAC Mech. Syst.*, vol. 33, no. 26, pp. 197–202, 2000, doi: 10.1016/S1474-6670(17)39144-9.

[19] G. Jose, R. Pascal, and V. Ioannis, "Tug boat propulsion system design and optimization," in *Proc. Int. Symp. Mar. Eng. (ISME)*, 2017, pp. 314–320.

[20] V. D. Hertog, K. Harford, and R. Stapleton, "RAptures: Resolving the tug-boat energy equation," in *Proc. Tugnology*, Amsterdam, The Netherlands, 2009, pp. 19–20.

[21] G. G. Dimopoulos, C. A. Georgopoulou, I. C. Stefanatos, A. S. Zymaris, and N. M. P. Kakalis, "A general-purpose process modelling framework for marine energy systems," *Energy Convers. Manage.*, vol. 86, pp. 325–339, Oct. 2014.

[22] T. I. Bo, A. R. Dahl, T. A. Johansen, E. Mathiesen, M. R. Miyazaki, E. Pedersen, R. Skjetne, A. J. Sorensen, L. Thorat, and K. K. Yum, "Marine vessel and power plant system simulator," *IEEE Access*, vol. 3, pp. 2065–2079, 2015, doi: 10.1109/ACCESS.2015.2496122.

[23] E. K. Dedes, D. A. Hudson, and S. R. Turnock, "Assessing the potential of hybrid energy technology to reduce exhaust emissions from global shipping," *Energy Policy*, vol. 40, pp. 204–218, Jan. 2012, doi: 10.1016/j.enpol.2011.09.046.

[24] M. R. Miyazaki, A. J. Sorensen, N. Lefebvre, K. K. Yum, and E. Pedersen, "Hybrid modeling of strategic loading of a marine hybrid power plant with experimental validation," *IEEE Access*, vol. 4, pp. 8793–8804, 2016, doi: 10.1109/ACCESS.2016.2629000.

[25] O. Simmonds, "DC: Is it the alternative choice for naval power distribution?" *J. Mar. Eng. Technol.*, vol. 13, no. 3, pp. 37–43, Dec. 2014, doi: 10.1080/20464177.2014.11658120.

[26] S. Castellan, R. Menis, A. Tessarolo, F. Luise, and T. Mazzuca, "A review of power electronics equipment for all-electric ship MVDC power systems," *Int. J. Electr. Power Energy Syst.*, vol. 96, pp. 306–323, Mar. 2018, doi: 10.1016/j.ijepes.2017.09.040.

[27] M. Chai, D. R. Bonthapalle, L. Sobrayen, S. K. Panda, D. Wu, and X. Chen, "Alternating current and direct current-based electrical systems for marine vessels with electric propulsion drives," *Appl. Energy*, vol. 231, pp. 747–756, Dec. 2018, doi: 10.1016/j.apenergy.2018.09.064.

[28] P. C. Krause, O. Wasynczuk, and S. D. Sudhoff, *Analysis of Electric Machinery and Drive Systems*, 3rd ed. New York, NY, USA: McGraw-Hill, Feb. 2013.

[29] J. Prousalidis, G. Antonopoulos, P. Mouzakis, and E. Sofras, "On resolving reactive power problems in ship electrical energy systems," *J. Mar. Eng. Technol.*, vol. 14, no. 3, pp. 124–136, Sep. 2015, doi: 10.1080/20464177.2015.1118786.

[30] J. M. Prousalidis, "The necessity of reactive power balance in ship electric energy systems," *J. Mar. Eng. Technol.*, vol. 10, no. 1, pp. 37–47, Jan. 2011, doi: 10.1080/20464177.2011.11020242.

[31] *Rotating Electrical Machines—Part 2-1: Standard Methods for Determining Losses and Efficiency From Tests (Excluding Machines for Traction Vehicles)*, document IEC 60034-2-1, 2014.

[32] S. Shisha and C. Sadarangani, "Testing and simulation for loss evaluation in field wound synchronous motors driven by voltage source inverters," in *Proc. Int. Conf. Electr. Mach. Syst.*, Nov. 2009, pp. 1–4, doi: 10.1109/ICEMS.2009.5382830.

[33] G. Traxler-Samek, R. Zickermann, and A. Schwery, "Cooling airflow, losses, and temperatures in large air-cooled synchronous machines," *IEEE Trans. Ind. Electron.*, vol. 57, no. 1, pp. 172–180, Jan. 2010, doi: 10.1109/TIE.2009.2031191.

[34] P. Rasilo, A. Belahcen, and A. Arkkio, "Experimental determination and numerical evaluation of core losses in a 150-kVA wound-field synchronous machine," *IET Electr. Power Appl.*, vol. 7, no. 2, pp. 97–105, Feb. 2013, doi: 10.1049/iet-epa.2012.0242.

[35] A. Frias, A. Kedous-Lebouc, C. Chillet, L. Albert, and L. Calegari, "Improvement and validation of an iron loss model for synchronous machine," in *Proc. 20th Int. Conf. Electr. Mach.*, Sep. 2012, pp. 1328–1332, doi: 10.1109/ICElMach.2012.6350049.

[36] A. E. Fitzgerald, C. Kingsley, Jr., and D. S. Umans, *Electric Machinery*, 5th ed. New York, NY, USA: McGraw-Hill, 2003, pp. 569–573.

[37] S. Pintz and J. Pospisil, "Equivalent loss energy methods of temperature testing synchronous machinery," *IEEE Trans. Power App. Syst.*, vol. PAS-99, no. 4, pp. 1691–1698, Jul. 1980.

[38] S. B. Guru and R. H. Hiziroglu, *Electric Machinery and Transformers* 3th ed. London, U.K.: Oxford Univ. Press, 2001, pp. 109–113.

[39] *Petroleum Measurement Tables—Part 1: Tables Based on Reference Temperatures of 15 Degrees C and 60 Degrees F*, document ISO 91-1, 1992.

[40] E. G. Giakoumis and A. I. Alafouzos, "Study of diesel engine performance and emissions during a transient cycle applying an engine mapping-based methodology," *Appl. Energy*, vol. 87, no. 4, pp. 1358–1365, Apr. 2010, doi: 10.1016/j.apenergy.2009.09.003.

[41] U. Hammarström, "10.4 research of heavy duty vehicle emissions and fuel consumption in Sweden," in *Emissions and Fuel Consumption From Heavy Duty Vehicles; COST 346-Final Report*. European Commission Transport Research and Innovation Monitoring and Information System, 2009, pp. 61–63. [Online]. Available: https://trimis.ec.europa.eu/project/emissions-and-fuel-consumption-heavy-duty-vehicles%C2%A0

[42] C. Ericson, B. Westerberg, and R. Egnell, "Transient emission predictions with quasi stationary model," in *Proc. Powertrain & Fluid Syst. Conf. Exhibit.*, San Antonio, TX USA, Oct. 2005, doi: 10.4271/2005-01-3852.
[43] K. K. Yum, N. Lefebvre, and E. Pedersen, "An experimental investigation of the effects of cyclic transient loads on a turbocharged diesel engine," *Appl. Energy*, vol. 185, pp. 472–481, Jan. 2017, doi: 10.1016/j.apenergy.2016.10.138.
[44] *Reciprocating Internal Combustion Engines—Performance—Part 1: Declarations of Power, Fuel and Lubricating Oil Consumptions, and Test Methods—Additional Requirements for Engines for General Use*, document ISO 3046-1, 2002.

HIROYASU KIFUNE (Member, IEEE) received the master's degree in mercantile marine from the Tokyo University of Mercantile Marine, Tokyo, Japan, in 2000, and the Ph.D. degree in electrical engineering from Yamaguchi University, Yamaguchi, Japan, in 2004.

He is currently an Associate Professor with the Department of Marine Electronics and Mechanical Engineering, Tokyo University of Marine Science and Technology. He used to research high-frequency inverters and their applications. His research interests include the power train systems, power management, and fuel saving of large vessels.

MEHDI KARBALAYE ZADHE (Member, IEEE) received the degree from the University of Tehran, Tehran, Iran, in 2010, and the Ph.D. degree in electrical engineering from the Norwegian University of Science and Technology, Trondheim, Norway, in 2016. From 2016 to 2017, he was with the power electronics industry, working on the development of battery charging systems. In 2017, he joined the Marine Technology Centre at NTNU, where he is currently an Associate Professor of hybrid power systems and the Director of the Marine Electrification Research Laboratory. His main research interests include ship electrification for low-emission and autonomous shipping, onboard DC power systems, and offshore renewable energy systems.

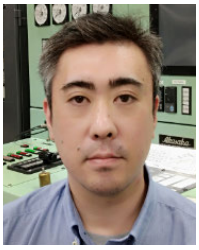

HIDETSUGU SASAKI received the master's degree in mercantile marine science from the Tokyo University of Mercantile Marine, Tokyo, Japan, in 2004, and the Ph.D. degree in mechanical engineering from The University of Tokyo, Tokyo, Japan, in 2017. He was a Research Engineer with TONETS Corporation, Tokyo, from 2004 to 2009. His research project was the development of HVAC systems. He joined the Tokyo University of Marine Science and Technology as a Research Assistant, since 2009. He is currently an Assistant Professor. His current research interests include the particulate matter measuring methodology for exhaust gas from marine diesel engines, particulate matter emission reduction, and electrostatic precipitator for marine diesel engines.